Human Molecular Genetics, 2016, Vol. 25, No. 2 275–290

doi: 10.1093/hmg/ddv470
Advance Access Publication Date: 18 November 2015
Original Article

ORIGINAL ARTICLE

Yeast reveals similar molecular mechanisms underlying alpha- and beta-synuclein toxicity

Sandra Tenreiro[1,2,*], Rita Rosado-Ramos[1], Ellen Gerhardt[3], Filippo Favretto[4], Filipa Magalhães[1], Blagovesta Popova[5,6], Stefan Becker[7], Markus Zweckstetter[4,7,8], Gerhard H. Braus[5,6] and Tiago Fleming Outeiro[2,4,6,*]

[1]Instituto de Medicina Molecular, Lisboa, Portugal, [2]CEDOC – Chronic Diseases Research Center, Faculdade de Ciências Médicas, Universidade Nova de Lisboa, Lisboa, Portugal, [3]Department of NeuroDegeneration and Restorative Research, University Medical Center Göttingen, Göttingen, Germany, [4]German Center for Neurodegenerative Diseases (DZNE), 37077 Göttingen, Germany, [5]Department of Molecular Microbiology and Genetics, Institute of Microbiology & Genetics, Georg-August-Universität Göttingen, Göttingen, Germany, [6]Center for Nanoscale Microscopy and Molecular Physiology of the Brain (CNMPB), Göttingen, Germany, [7]Department of NMR-Based Structural Biology, Max Planck Institute for Biophysical Chemistry, Am Fassberg 11, 37077 Göttingen, Germany and [8]DFG Research Center for Nanoscale Microscopy and Molecular Physiology of the Brain (CNMPB), University Medical Center Göttingen, 37073 Göttingen, Germany

*To whom correspondence should be addressed at: CEDOC – Chronic Diseases Research Center, Faculdade de Ciências Médicas, Universidade Nova de Lisboa, Rua Câmara Pestana n° 6, Edifício CEDOC II, 1150-082 Lisboa, Portugal. Tel: +351 218803101; Fax: +351 218803010; Email: stenreiro@nms.unl.pt (S.T.); Department of NeuroDegeneration and Restorative Research, University Medical Center Gottingen, Waldweg 33, 37073 Gottingen, Germany. Tel: +49 5513913544; Fax: +49 5513922693; Email: touteir@gwdg.de (T.F.O.)

Abstract

Synucleins belong to a family of intrinsically unstructured proteins that includes alpha-synuclein (aSyn), beta-synuclein (bSyn) and gamma-synuclein (gSyn). aSyn is the most studied member of the synuclein family due to its central role in genetic and sporadic forms of Parkinson's disease and other neurodegenerative disorders known as synucleionopathies. In contrast, bSyn and gSyn have been less studied, but recent reports also suggest that, unexpectedly, these proteins may also cause neurotoxicity. Here, we explored the yeast toolbox to investigate the cellular effects of bSyn and gSyn. We found that bSyn is toxic and forms cytosolic inclusions that are similar to those formed by aSyn. Moreover, we found that bSyn shares similar toxicity mechanisms with aSyn, including vesicular trafficking impairment and induction of oxidative stress. We demonstrate that co-expression of aSyn and bSyn exacerbates cytotoxicity, due to increased dosage of toxic synuclein forms, and that they are able to form heterodimers in both yeast and in human cells. In contrast, gSyn is not toxic and does not form inclusions in yeast cells. Altogether, our findings shed light into the question of whether bSyn can exert toxic effects and confirms the occurrence of aSyn/bSyn heterodimers, opening novel perspectives for the development of novel strategies for therapeutic intervention in synucleinopathies.

Received: July 7, 2015. **Revised and Accepted:** November 10, 2015

Introduction

The synuclein family consists of three intrinsically unstructured proteins: alpha-synuclein (aSyn) and beta-synuclein (bSyn), which are widely expressed in the central nervous system including neocortex, hippocampus, striatum, thalamus and cerebellum, and gamma-synuclein (gSyn), which is predominantly expressed in the peripheral nervous system (1).

The precise function of these three vertebrate-specific proteins is unclear. Triple knockout mice exhibit a mild phenotype with alterations in synaptic structure and transmission, age-dependent neuronal dysfunction, as well as reduced survival (2). Recently, synucleins were reported to play a role in the early steps of synaptic vesicle endocytosis, showing some degree of functional redundancy (3). The three proteins share a highly conserved N-terminal domain and a less-conserved C-terminal region (4). Human aSyn is 140 amino acids while bSyn is 134 amino acids long. The two proteins share 61% sequence homology. gSyn is 127 amino acids long and shares 55.9 and 54.3% sequence homology with aSyn and bSyn, respectively (1,5). The region of highest homology between the three synuclein proteins is the N-terminal region.

aSyn is the most studied member of the family due to its genetic association with familial and sporadic forms of Parkinson's disease (PD). aSyn is also the major component of protein inclusions known as Lewy bodies (LBs) or Lewy neurites (LNs), typical pathological hallmark inclusions in PD and other neurodegenerative disorders known as synucleinopathies (6).

bSyn and gSyn do not seem to be present in LBs (7), and have not been strongly linked to synucleinopathies. However, a recent study revealed bSyn can also induce dopaminergic cell loss when expressed in rat brain (8), challenging initial reports suggesting it could act as a scavenger of aSyn aggregation and neurotoxicity, in several *in vivo* and *in vitro* models (9–12).

bSyn was thought to be less prone to aggregation than aSyn since it lacks part of the non-β-amyloid component (NAC) region, known to be important for aggregation. However, in particular conditions such as exposure to metal ions, macromolecular crowding and pesticides, aggregation and fibrillation of bSyn can be induced (13). Moreover, V70M and P123H mutations in bSyn were associated with rare cases of dementia with LBs (DLBs) (14). When overexpressed in a neuroblastoma cell line, these mutations induced the formation of lysosomal inclusions, an effect that was enhanced by co-expression with aSyn (15). Also, overexpression of aSyn exacerbated the progressive neurodegeneration of transgenic mice expressing P123H bSyn (16). Stronger evidence of a neuropathological role of bSyn was recently described in a study where wild-type (WT) human bSyn was found to be neurotoxic in primary neuronal cultures and when expressed in the rat substantia nigra (8).

gSyn was associated with tumor progression and metastasis in a wide variety of cancers such as breast cancer, ovarian and brain tumors (17,18), and also with neurodegenerative and ocular diseases (19). Abnormal structures positive for gSyn were reported in brains of some patients with PD, DLB and Hallervorden–Spatz syndrome (20,21). More recently, gSyn-positive inclusions were found in the cell bodies and/or in the axonal compartment of the affected motor neurons of 30% of amyotrophic lateral sclerosis (ALS) patients (22).

Several posttranslational modifications (PTMs) of aSyn were found to modulate neurotoxicity, such as phosphorylation, oxidation and nitration (23–26). Among them, phosphorylation is the most studied, as 90% of the aSyn aggregated in LBs was found to be phosphorylated on serine 129 (S129) (27,28). Additional phosphorylation sites in aSyn have been identified and studied [Y39, S87, Y125, Y133 and Y136 (29)]. However, although distinct aSyn phosphorylation patterns were observed in synucleinopathies (30,31), the precise effect of phosphorylation on aSyn aggregation and toxicity is still unclear.

PTMs in bSyn and gSyn are less studied than those in aSyn. bSyn was originally described as a phosphoprotein that undergoes phosphorylation both *in vitro* and *in vivo* (32). Although the human Polo-like kinases (PLKs) 2 and 3 were found to phosphorylate bSyn at serine 118 (S118), it is still unclear whether this modification plays a role in pathology (5).

Saccharomyces cerevisiae has been widely used to study the basic molecular mechanisms underlying various neurodegenerative diseases (33). Here, we used yeast as an unbiased living test tube to interrogate the intrinsic cytotoxicity of the three synuclein family members, and to dissect the molecular mechanisms of toxicity. We found that, like aSyn, bSyn is toxic and forms inclusions. In contrast, gSyn is not toxic and does not form inclusions. We found that the cellular pathways affected by bSyn are similar to those affected by aSyn, including impairment of vesicular trafficking and induction of oxidative stress. Interestingly, we demonstrate that co-expression of aSyn and bSyn exacerbates cytotoxicity, due to increased gene dosage, and that these two synucleins form heterodimers in both yeast and in human human embryonic kidney (HEK) cells.

Altogether, our study provides novel insight into the molecular effects of the three synuclein family members, establishing the basis for future studies that may impact on our understanding of synucleinopathies.

Results

bSyn is toxic and forms inclusions when expressed in yeast cells

In order to evaluate whether human bSyn and gSyn affected yeast cell growth, we expressed these proteins, fused with GFP, in multi-copy plasmids using a galactose-inducible promoter (*GAL1*) (Table 1). Growth was assessed using a spotting assay and compared with the strain containing the empty vector as a control (Fig. 1A). As described before (35), expression of aSyn in yeast cells is toxic and results in reduced cell growth (Fig. 1A). However, cells expressing bSyn also displayed reduced growth compared with control cells, suggesting that the expression of this synuclein is also toxic (Fig. 1A). Cells expressing gSyn presented similar growth to the control cells, indicating that this synuclein is not toxic in yeast (Fig. 1A). To investigate whether the growth defect was due to cytotoxicity, these results were further confirmed by propidium iodide (PI) staining and flow cytometry analysis of cells where plasma membrane integrity was compromised (Fig. 1B). In fact, 6 h after induction of expression, 20.4 ± 1% of the yeast cells expressing aSyn-GFP and 16.3 ± 1.4% of the yeast cells expressing bSyn-GFP were PI positive, compared with only 4.3 ± 1.4% of cells containing the empty vector, or 7.8 ± 3.0% of cells expressing gSyn (non-significant) (Fig. 1B).

We next assessed the correlation between cytotoxicity and the subcellular distribution of synuclein proteins. Cells expressing aSyn, bSyn or gSyn fused to GFP were analyzed by fluorescence microscopy, and the percentage of cells displaying inclusions was counted (Fig. 1C). As reported before, aSyn expression in yeast leads to the formation of cytoplasmic inclusions (35). In our experimental conditions, we found 42 ± 6.1% of the cells displayed aSyn inclusions. Interestingly, cells expressing bSyn-GFP

Table 1. Yeast plasmids used in this study

Plasmid	Type	Source
p426Gal	Multicopy	(34)
p423Gal	Multicopy	(34)
p425Gal	Multicopy	(34)
p425Gal-aSyn-GFP	Multicopy	(35)
p426Gal-aSyn-GFP	Multicopy	(35)
p425Gal-bSyn-GFP	Multicopy	This study
p426Gal-bSyn-GFP	Multicopy	This study
p425Gal-gSyn-GFP	Multicopy	This study
p426Gal-gSyn-GFP	Multicopy	This study
p426Gal-gSyn S118D-GFP	Multicopy	This study
p426Gal-gSyn S118A-GFP	Multicopy	This study
p426Gal-gSyn S118G-GFP	Multicopy	This study
p426Gal-gSyn V70M-GFP	Multicopy	This study
p426Gal-gSyn P123H-GFP	Multicopy	This study
p426Gal-GFP	Multicopy	This study
p426Gal-VN-aSyn	Multicopy	This study
p426Gal-VN-bSyn	Multicopy	This study
p426Gal-VN-gSyn	Multicopy	This study
p423Gal-aSyn-VC	Multicopy	This study
p423Gal-bSyn-VC	Multicopy	This study
p423Gal-gSyn-VC	Multicopy	This study

also presented cytoplasmic inclusions (22.4 ± 4.2%). In contrast, no inclusions were visible in the cells expressing gSyn-GFP. As with aSyn, both bSyn-GFP and gSyn-GFP were present at the plasma membrane and in the cytosol (Fig. 1C). We next asked whether the differences in toxicity and inclusion formation were due to different expression levels of the different synuclein homologs. Using immunoblot analyses, we found bSyn-GFP and gSyn-GFP were expressed at similar levels with aSyn-GFP (Fig. 1D).

Given that only bSyn formed inclusions and induced cytotoxicity, we focused the study on this synuclein. To evaluate if the inclusions formed by aSyn-GFP or bSyn-GFP have similar dynamic properties, we used fluorescence recovery after photobleaching (FRAP), an assay we have previously employed for characterizing aSyn inclusions (36). Interestingly, we found that inclusions formed by aSyn-GFP and bSyn-GFP present similar FRAP recovery profiles, demonstrating these inclusions display comparable protein immobile fractions and mean residence time (Fig. 1E).

aSyn expression in yeast cells induces oxidative stress by increasing reactive oxygen species (ROS) production (37), and by affecting mitochondria function (38). Thus, we compared the intracellular levels of superoxide radical in cells expressing aSyn or bSyn using dihydroethidium (DHE) and flow cytometry (Fig. 1F). As expected, the expression of aSyn in yeast cells leads to the increase of superoxide radical levels (39). We observed that the expression of bSyn in yeast cells also results in a significant increase in the levels of superoxide radical (Fig. 1F).

Altogether, these results demonstrate that bSyn expression in yeast cells is toxic and forms inclusions that are similar to those formed by aSyn. In contrast, gSyn is not toxic and does not form inclusions at the levels of expression tested.

bSyn promotes endoplasmic reticulum-to-Golgi trafficking defects in yeast

Several studies showed that aSyn disrupts multiple intracellular trafficking pathways, such as endoplasmic reticulum (ER)-to-Golgi trafficking (40). Interestingly, genes that promote ER-to-Golgi trafficking rescue aSyn toxicity, while genes that negatively regulate ER-to-Golgi trafficking enhance aSyn toxicity (40). To evaluate if bSyn toxicity is also associated with ER-to-Golgi trafficking impairment, we tested the effects of previously described suppressors (Ypt1, Ykt6 and Ubp3) and enhancers (Gyp8 and Pmr1) of aSyn toxicity on bSyn toxicity (36,40). Both types of genetic modifiers were co-expressed with aSyn-GFP or bSyn-GFP and the effect on toxicity and inclusion formation was evaluated 6 h after expression induction (Fig. 2). Although the co-expression of Ypt1, Ykt6 and Ubp3 significantly reduced the toxicity of aSyn and bSyn (Fig. 2A), no significant differences in inclusion formation were observed (Fig. 2B). In contrast, co-expression of Gyp8 or, to a lesser extent, Pmr1, significantly increased toxicity and inclusions formation of aSyn and bSyn (Fig. 2B).

We also evaluated if the enhancers of aSyn and bSyn toxicity (Gyp8 and Pmr1) could enhance gSyn toxicity, but found no effect (Supplementary Material, Fig. S1A). Moreover, neither gene modified gSyn-GFP inclusion formation (Supplementary Material, Fig. S1B).

To exclude that the phenotypes observed resulted from an effect of the modifiers on the expression levels of the synuclein proteins, we preformed western blot analyses. We found that total aSyn, bSyn and gSyn levels were not significantly affected by the co-expression of the genetic modifiers (Fig. 2C and Supplementary Material, Fig. S1C).

Altogether, these results indicate that bSyn is also associated with ER-to-Golgi trafficking defects. In contrast, gSyn is not toxic even when vesicle trafficking defects are genetically induced.

V70m and P123H bSyn mutations increase inclusion formation without affecting toxicity

Sporadic and familial cases of DLBs were previously associated with the point mutations V70M and P123H in bSyn, respectively (14). Here, we analyzed the effect of these mutations on bSyn toxicity and inclusion formation yeast (Fig. 3). Interestingly, while V70M and P123H mutations had no effect on bSyn toxicity (Fig. 3A), the percentage of cells with inclusions was 2-fold higher (~40%) that that of cells expressing WT bSyn (~20%) (Fig. 3B).

We next evaluated the effect of V70M and P123H mutations on the levels of expression of bSyn-GFP. Using immunoblot analyses, we observed all three variants of bSyn were expressed at similar levels after 6 h of expression induction (Fig. 3C).

The phospho-mimic mutation S118D increases bSyn toxicity and inclusion formation

bSyn is phosphorylated by PLK2 and 3 on serine 118 (S118) (5). However, it is not known if this PTM has a pathological role. Thus, we addressed this question using mutants that either mimic (S118D) or block phosphorylation (S118A or S118G). Cells expressing the S118D mutant exhibited a more severe growth defect phenotype, while cells expressing the S118A or S118G mutants behaved as those expressing WT bSyn (Fig. 4A). We then assessed the correlation between cytotoxicity and the subcellular distribution of S118D, S118A and S118G aSyn-GFP, by fluorescence microscopy. While we found no different in the percentage of cells displaying inclusions between the different variants of bSyn (data not shown), we found that cells expressing the phospho-mimic S118D mutation presented a significant increase in the number of inclusions per cell (Fig. 4B). We next assessed whether the differences in toxicity and inclusion formation were due to different expression levels of the variants of bSyn-GFP. Using immunoblot analyses, we observed that all variants were expressed at similar levels after 6 h of expression induction (Fig. 4C).

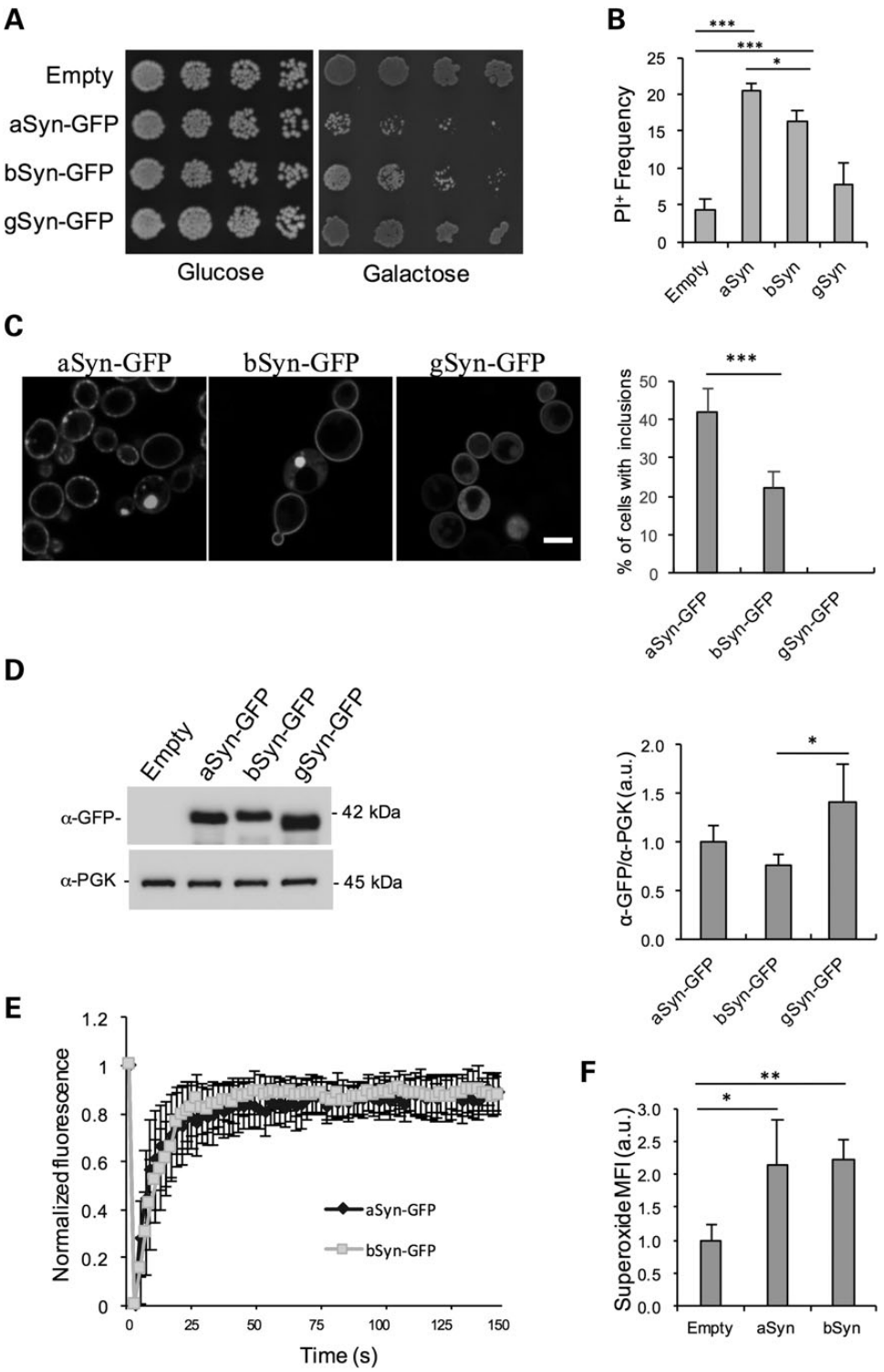

Figure 1. bSyn is toxic and forms inclusions in yeast cells. (A) Cytotoxicity of aSyn, bSyn and gSyn in yeast cells compared with the empty vector, assessed by spotting assay. Photos were taken 4 days after incubation at 30°C (B) Frequency of PI positive cells assessed by flow cytometry, after 6 h of induction of expression of the different synuclein proteins. (C) Fluorescence microscopy visualization (left panel) and percentage of cells with aSyn or bSyn inclusions (right panel). (D) Expression levels of aSyn, bSyn and gSyn-GFP in yeast cells assessed by western blot analysis of total protein extracts (left panel). Densitometric analysis of the immunodetection of GFP relative to the intensity obtained for PGK used as loading control presented in arbitrary units (a.u.) (right panel). (E) FRAP recovery curves for aSyn and bSyn-GFP inclusions on yeast cells. For each strain, at least six inclusions in different cells were analyzed. Each plot represents mean ± SD for each time point for all FRAP experiments. (F) Superoxide radical levels in yeast cells expressing either aSyn or bSyn after 24 h of expression induction, assessed by flow-cytometry using the DHE probe. Results shown are from one representative experiment from at least three independent experiments. Values represent the mean ± SD of at least three independent measurements (***$P < 0.001$, **$P < 0.01$, *$P < 0.05$).

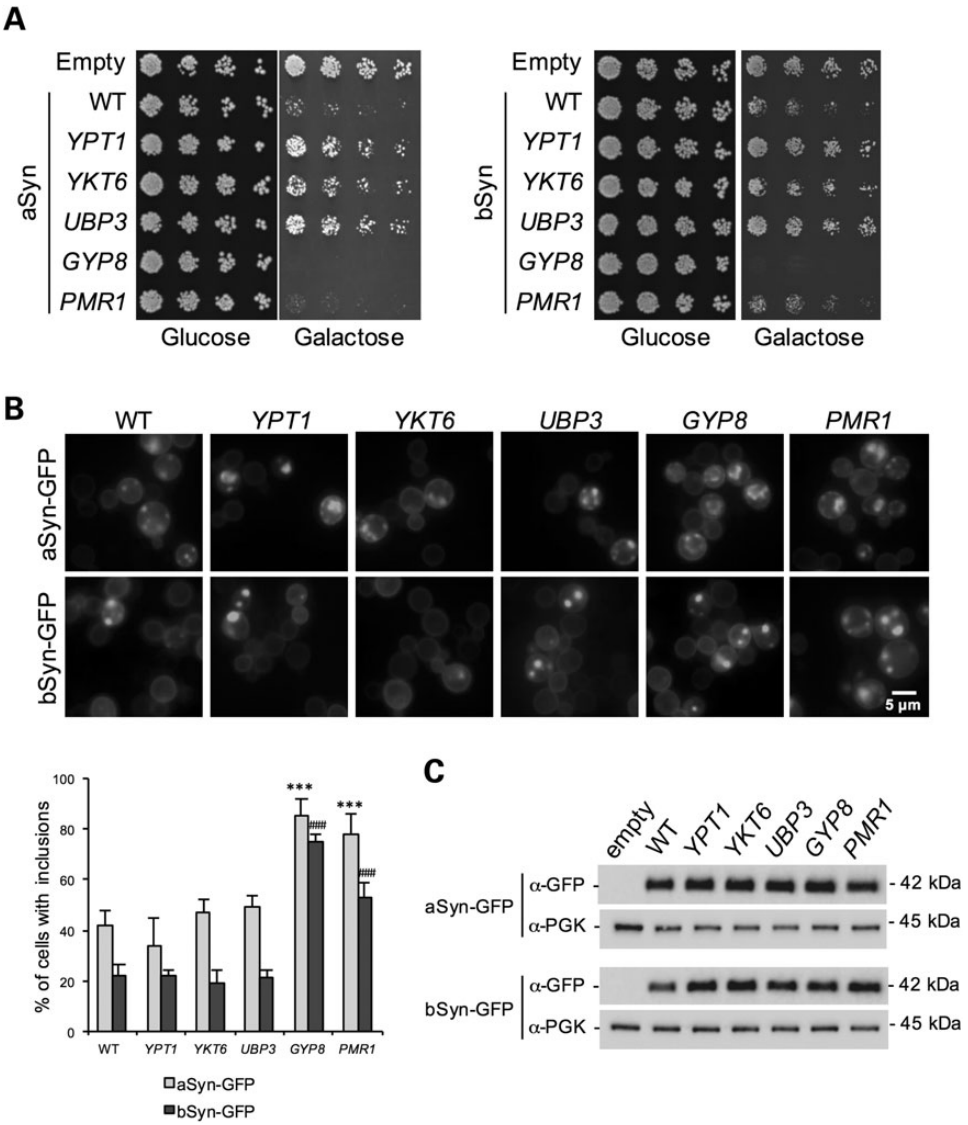

Figure 2. Vesicular trafficking genes as modifiers of bSyn toxicity. (**A**) Spotting assay of the indicated yeast cells. Photos were taken 3 days after incubation at 30°C (**B**) Intracellular localization of aSyn and bSyn-GFP (upper panel) and percentage of yeast cells containing inclusions (lower panel) in the indicated yeast strains, assessed by fluorescence microscopy after 6 h of expression induction. Values represent the mean ± SD (***$P < 0.001$ versus WT; ###< 0.001 versus aSyn). (**C**) aSyn, bSyn and gSyn-GFP expression levels in the indicated yeast strains assessed by western blot analysis of total protein. A representative result is shown from at least three independent experiments.

Overall, these results indicate that phosphorylation of bSyn at S118 might contribute to toxicity and inclusions formation in yeast cells.

Co-expression of aSyn and bSyn increases toxicity and inclusion formation

Next, we asked whether aSyn and bSyn altered each other's behavior in yeast cells. Upon co-expression of both proteins, we found that this resulted in a strong increase in toxicity, with complete lack of growth (Fig. 5A). To clarify if this phenotype was due to a synergistic or an additive effect, we used the same conditions and co-expressed aSyn plus aSyn and bSyn plus bSyn, using expression vectors with different auxotrophic markers. We found that co-expression of aSyn plus aSyn and bSyn plus bSyn also increased toxicity (Fig. 5A). Next, we evaluated cells where plasma membrane integrity was compromised using PI staining and flow cytometry analysis, 12 h after induction of expression (Fig. 5B). No significant differences were observed in the percentage of PI-positive cells when aSyn plus bSyn, aSyn plus aSyn or bSyn plus bSyn were co-expressed (Fig. 5B). Regarding the percentage of cells with inclusions, a slight but significant increase was observed when aSyn was co-expressed with bSyn, compared with aSyn plus aSyn or bSyn plus bSyn expressing cells, 6 h after expression induction (Fig. 5C).

In parallel, we also evaluated the effect of the co-expression of gSyn with aSyn and bSyn. We observed that co-expression of gSyn-GFP with aSyn-GFP or bSyn-GFP reduced the toxicity of both proteins, as assessed by spotting assay and by PI staining (Fig. 5A and B). Moreover, gSyn-GFP co-expression with aSyn-GFP or bSyn-GFP also reduced the percentage of cells with inclusions (Fig. 5C).

Next, we assessed whether the phenotypes observed were due to altered expression levels of the different synuclein proteins,

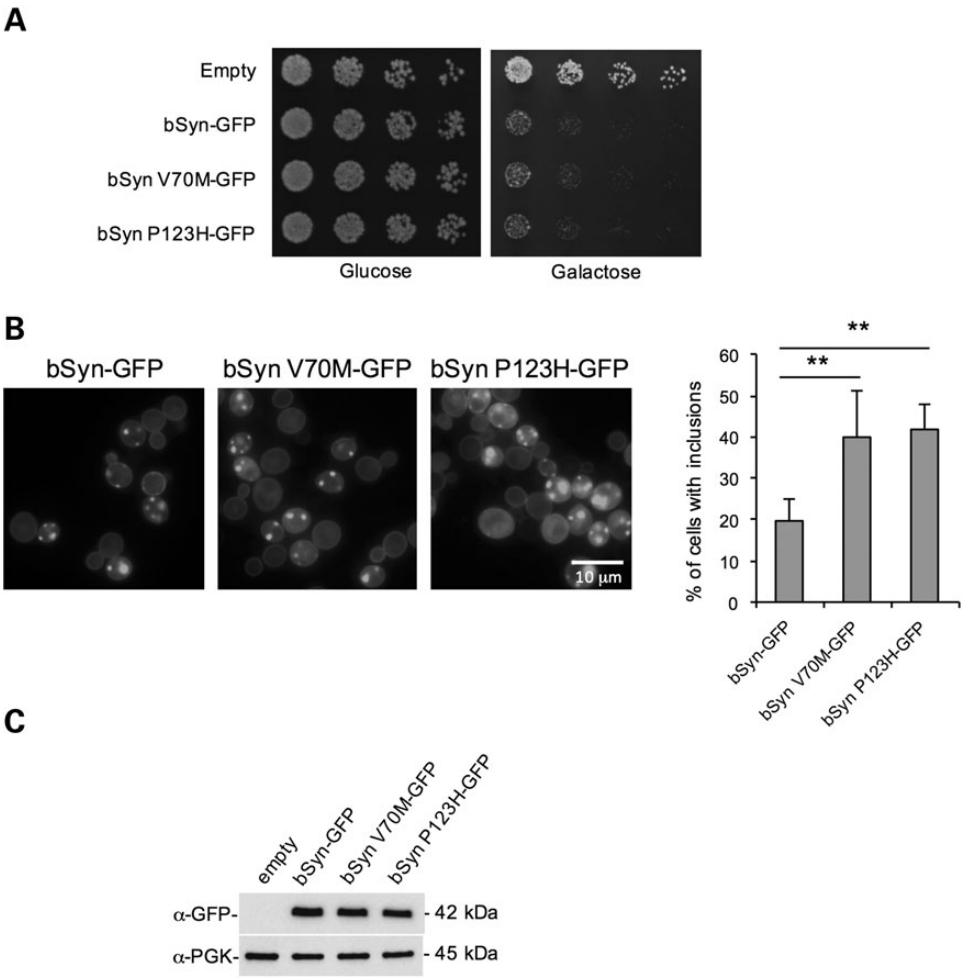

Figure 3. The effect of V70M and P123H mutations on bSyn inclusion formation and toxicity. (**A**) Cytotoxicity of WT, V70M or P123H bSyn expression in yeast cells compared with the empty vector assessed by spotting assay. Photos were taken 3 days after incubation at 30°C. (**B**) Fluorescence microscopy visualization (left panel) and percentage of cells with bSyn inclusions (right panel) after 6 h of expression induction. (**C**) Expression levels of aSyn, WT, V70M or P123H bSyn-GFP in yeast cells assessed by western blot analysis of total protein extracts. A representative result is shown from at least three independent experiments. Values represent the mean ± SD (**$P < 0.01$).

using immunoblot analyses (Fig. 5D). We observed that in the conditions tested, using multicopy expression vectors, the co-expression of synuclein proteins affected protein levels (Fig. 5D). Thus, this might contribute to an alleviation of the phenotypes observed. In particular, we observed that co-expression of aSyn or bSyn with gSyn-GFP resulted in reduced protein levels, accounting for the reduced toxicity and inclusion formation (Fig. 5D).

We then assessed whether aSyn, bSyn and gSyn were able to form heterodimers in yeast cells, taking advantage of the bimolecular fluorescence complementation assay (BiFC) (41). In this approach, aSyn, bSyn and gSyn were tagged with the N-terminal half of Venus (VN) or the C-terminal half of Venus (VC), respectively. In the BiFC assay, the occurrence of Venus fluorescence signal indicates the formation of at least dimeric species. As expected, we observed the formation of aSyn and bSyn dimers/oligomers (Fig. 6A). Interestingly, we not only observed the formation of aSyn/bSyn heterodimers, but also the formation of inclusions composed of both aSyn and bSyn (Fig. 6A). The intensity of the fluorescence signal was further evaluated by flow cytometry, revealing that the pair VN-aSyn/bSyn-VC is more competent in forming heterodimers/oligomers than the pair VN-bSyn/aSyn-VC (Fig. 6B). In addition, the cells expressing the pair VN-aSyn/bSyn-VC displayed lower mean fluorescence intensity (MFI) when compared with the pair VN-aSyn/aSyn-VC, but higher than the pair VN-bSyn/bSyn-VC, indicating an additive effect on the formation of heterodimers/oligomers when aSyn and bSyn were co-expressed (Fig. 6C).

We also evaluated the ability of gSyn to form heterodimers with aSyn and bSyn in yeast cells. We observed heterodimer formation just for one combination: VN-aSyn + gSyn-VC. Interestingly, the signal was only detected at the plasma membrane and we observed no inclusion formation. In all other combinations we found no fluorescent signal, suggesting the orientation of the proteins in the heterodimers does not enable the reconstitution of the functional fluorophore (Fig. 6 and Supplementary Material, Fig. S2).

Importantly, the differences observed when aSyn and bSyn were co-expressed were not due to different expression levels of the corresponding fusion proteins, as no significant differences were detected by immunoblot analysis (Fig. 6D).

aSyn and bSyn form heterodimers in both yeast and mammalian cell models

The formation of heterodimers between aSyn and bSyn had not been previously reported. Therefore, to confirm the data obtained

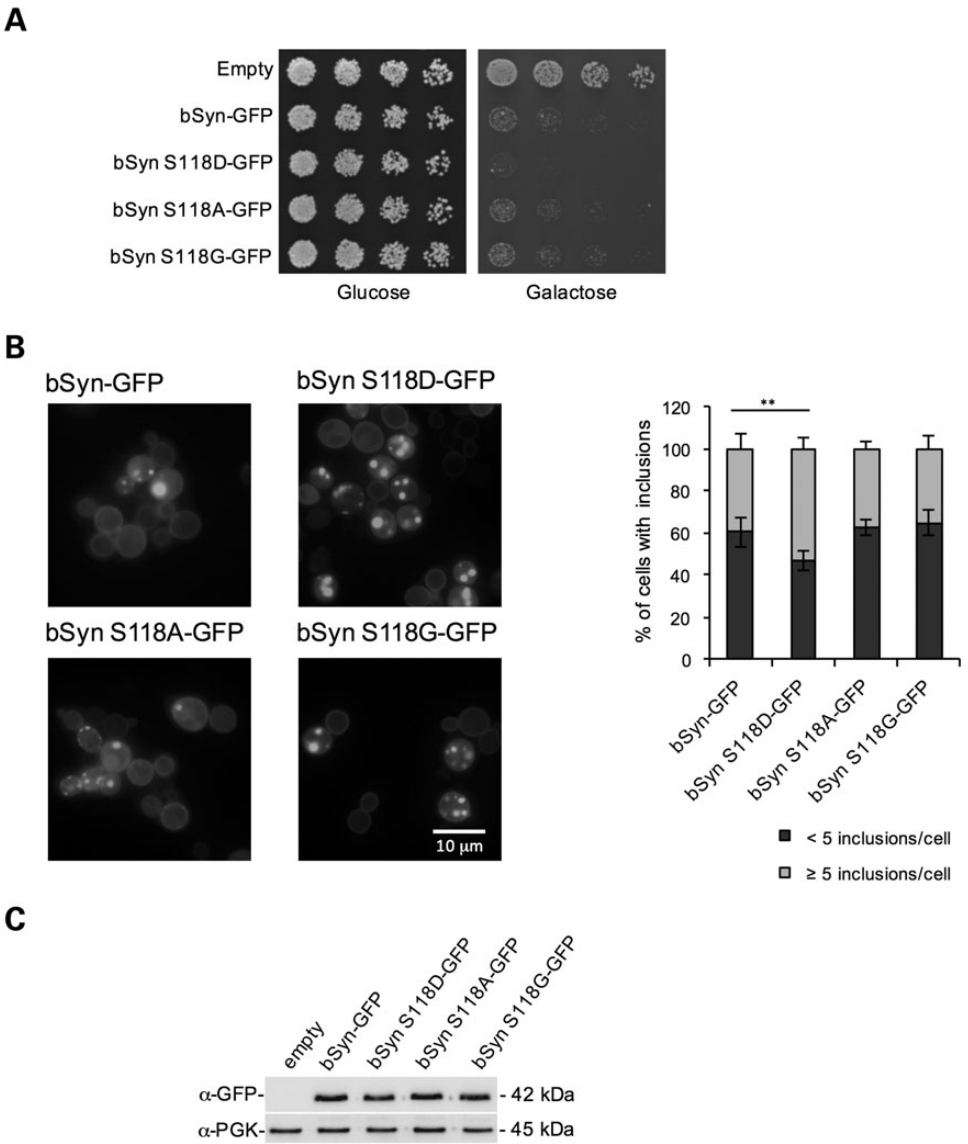

Figure 4. The effect of S118 phosphorylation on bSyn inclusion formation and toxicity. (**A**) Cytotoxicity of WT, S118D, S118A or S118G bSyn expression in yeast cells compared with the empty vector assessed by spotting assay. Photos were taken 3 days after incubation at 30°C. (**B**) Fluorescence microscopy visualization (left panel) and percentage of cells with bSyn inclusions (right panel) after 6 h of expression induction. The percentage of cells with <5 and with ≥5 inclusions per cell is represented (right panel). (**C**) Expression levels of WT, S118D, S118A or S118G bSyn-GFP in yeast cells assessed by western blot analysis of total protein extracts. A representative result is shown from at least three independent experiments. Values represent the mean ± SD (***$P < 0.001$, **$P < 0.01$).

in yeast, we performed the BiFC assay in HEK cells (HEK293). Cells were co-transfected with different combinations of the constructs encoding aSyn or bSyn fused to the N- or C-terminal fragments of Venus. We observed that both combinations of aSyn/bSyn constructs resulted in the formation of heterodimers, as observed in yeast cells (Fig. 7A).

Immunoblot analyses confirmed the expression of the various BiFC constructs was identical (Fig. 7B).

In order to confirm that untagged aSyn and bSyn behaved similarly to the BiFC constructs, we performed inmmunocytochemistry in cells transfected with aSyn, bSyn-V5, or aSyn + bSyn-V5. In cells co-expressing both proteins, the subcellular distribution pattern was identical, in agreement with the findings using the BiFC assay (Fig. 7C).

Altogether, we confirmed that aSyn and bSyn can form heterodimers in human cells, further supporting a possible additive effect toward pathology.

Monomeric aSyn and bSyn do not interact in solution

To evaluate if aSyn and bSyn heterodimer formation occurred during the aggregation process or was already initiated between the two monomeric proteins in solution, we performed nuclear magnetic resonance (NMR) spectroscopy. NMR spectroscopy is able to detect and quantify both strong and weak molecular interactions and provides residue resolution about the interaction. To this end, we labeled bSyn with ^{15}N and recorded a two-dimensional {^{1}H–^{15}N}-HSQC experiment, which provides a fingerprint of the backbone resonances of bSyn (Fig. 8A). Next, we tagged aSyn with the nitroxide-label S-(1-oxyl-2,2,5,5-tetramethyl-2,5-dihydro-1H-pyrrol-3-yl)methyl methanesulfonothioate (MTSL) at position 90, in order to increase the sensitivity of detection toward intermolecular interactions (42). In particular, because bSyn does not carry a paramagnetic center, any NMR signal broadening that would be observed upon addition of aSyn

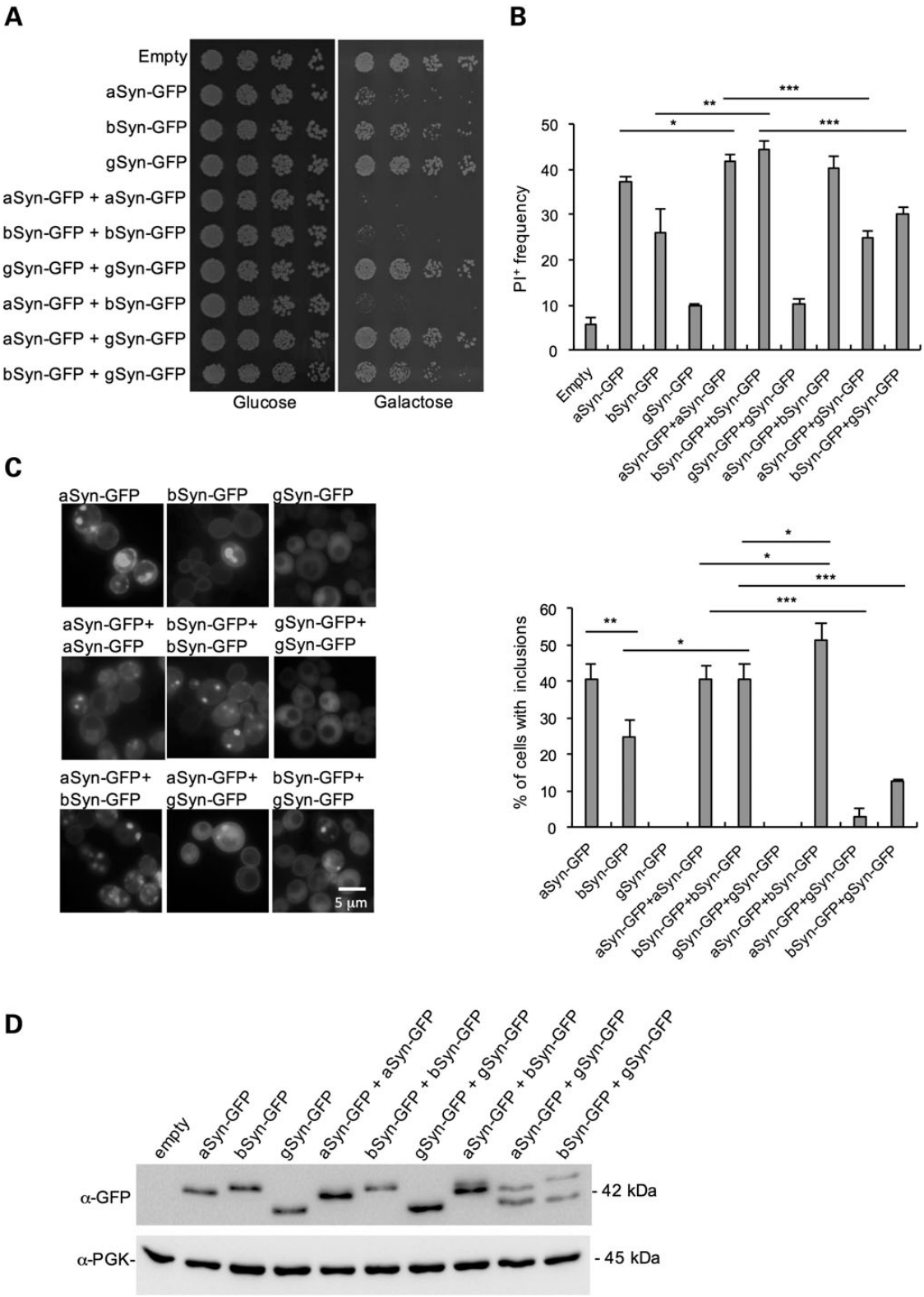

Figure 5. Co-expression of aSyn, bSyn and gSyn toxicity and inclusion formation in yeast cells. Co-expression of the different synuclein proteins was achieved using expression vectors with different auxotrophic markers. (**A**) Cytotoxicity of aSyn-GFP and bSyn-GFP, either alone or co-expressed in yeast cells compared with the empty vector and assessed by spotting assay. Pictures were taken 4 days after incubation at 30°C. (**B**) Frequency of PI positive cells assessed by flow cytometry, after 12 h of induction of expression of the different synuclein proteins in the indicated combinations. (**C**) Fluorescence microscopy visualization (left panel) and percentage of cells with inclusions expressing the indicated synuclein proteins (right panel), after 6 h of expression induction. (**D**) Expression levels of aSyn, bSyn and gSyn-GFP in the indicated yeast strains after 12 h of expression induction, assessed by western blot analysis of total protein extracts. A representative result is shown from at least three independent experiments. Values represent the mean ± SD (***$P < 0.001$, **$P < 0.01$ and *$P < 0.05$).

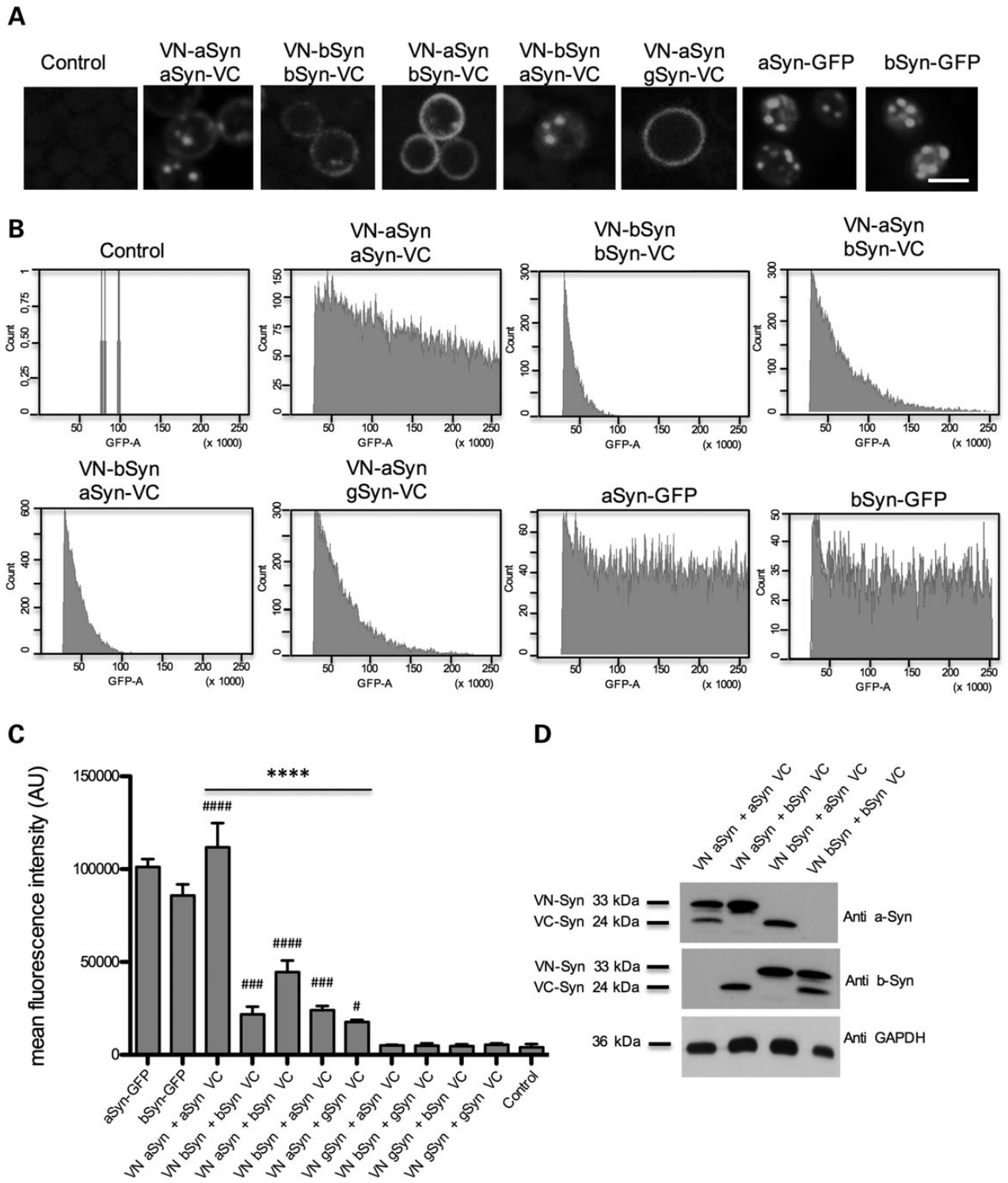

Figure 6. aSyn and bSyn form homo- and hetero-dimers/oligomers in yeast. Yeast cells were transformed with BiFC constructs encoding aSyn, bSyn or gSyn tagged with N-terminal half of Venus (VN) or C-terminal half of Venus (VC) under the control of *GAL1* inducible promoter. aSyn-GFP, bSyn-GFP and VN-aSyn + VC were used as controls. (**A**) Fluorescence microscopy after 6 h induction of synuclein expression, showing fluorescence complementation signal in living cells. Scale bar: 5 μm. (**B**) GFP intensity versus counts assessed by flow cytometry 6 h after synuclein expression induction. At least 100 000 cells were measured per strain and experiment. Results shown are from one representative experiment from three independent experiments. Control: transformation of yeast cells with VN-aSyn + VC; VN-bSyn + VC or VN-gSyn + VC does not result in positive fluorescence intensity, indicating that fluorescence is caused only by specific protein interactions. (**C**) Mean fluorescence intensity for the indicated plasmid combinations. The results are mean from three independent experiments ± SD. Significance of differences was calculated with one-way ANOVA with Bonferroni's multiple comparison test ($^{****}P < 0.0001$; $^{\#}P < 0.05$; $^{\#\#\#}P < 0.001$; $^{\#\#\#\#}P < 0.0001$ versus control). (**D**) Immunoblotting analysis of total protein extracts 6 h after induction of synuclein expression of transformants, used in the BiFC experiments.

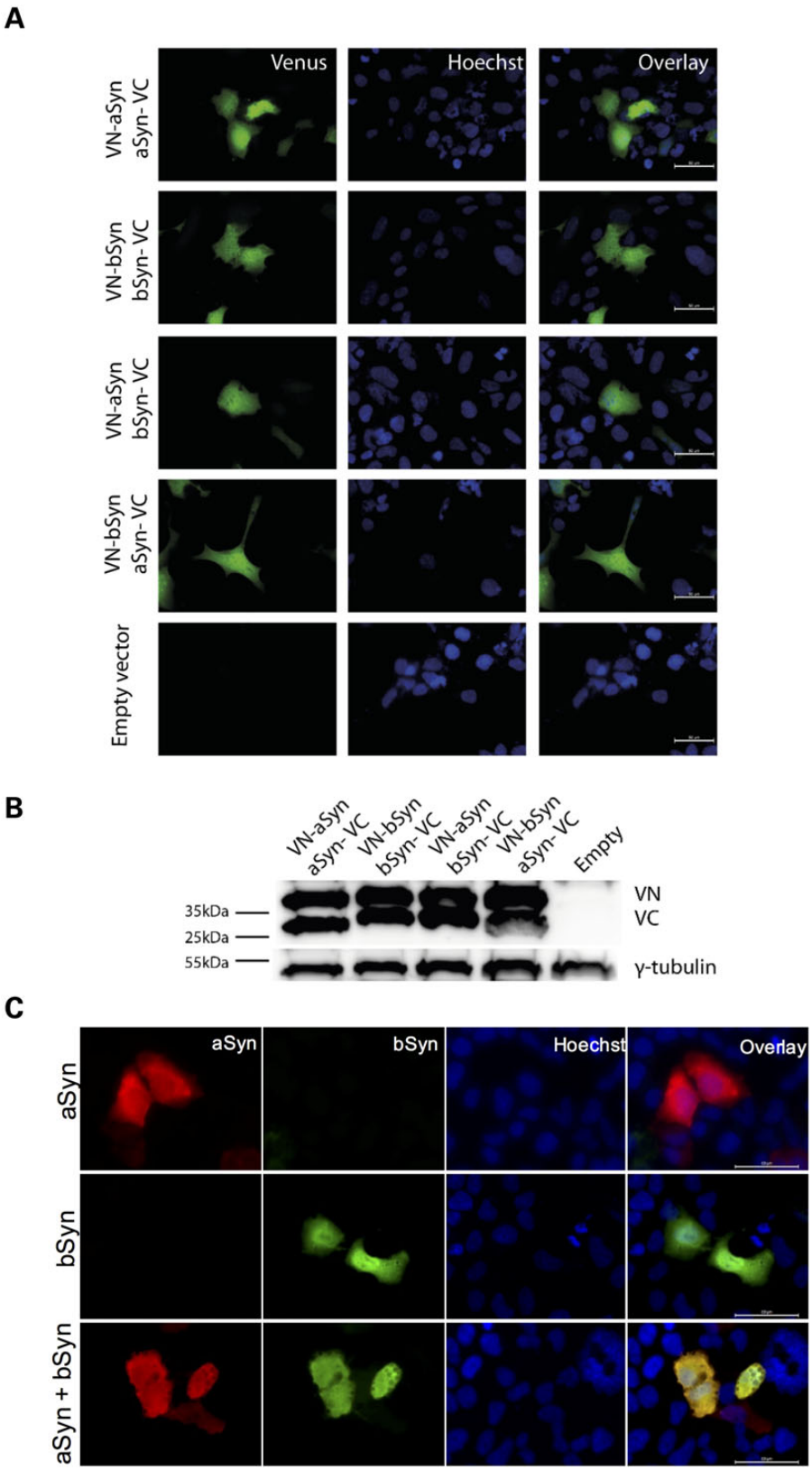

Figure 7. aSyn and bSyn form heterodimers in HEK293 cells. HEK293 cells were transfected with BiFC constructs encoding either aSyn or bSyn tagged with the N-terminal (VN) or C-terminal half of Venus (VC) under the control of the CMV promoter. (**A**) Fluorescence microscopy pictures 48 h after transfection. Scale bar: 50 μm. (**B**) Representative immunoblot to evaluate the levels of expression of the various constructs in HEK293 cells, showing aSyn and bSyn fused-to the VN- or VC-part, detected by using a pan-specific synuclein specific antibody, and the loading control. (**C**) Fluorescence microscopy of cells transfected with untagged aSyn, bSyn-V5, or aSyn + bSyn-V5 and stained with antibodies against either aSyn or the V5 epitope tag.

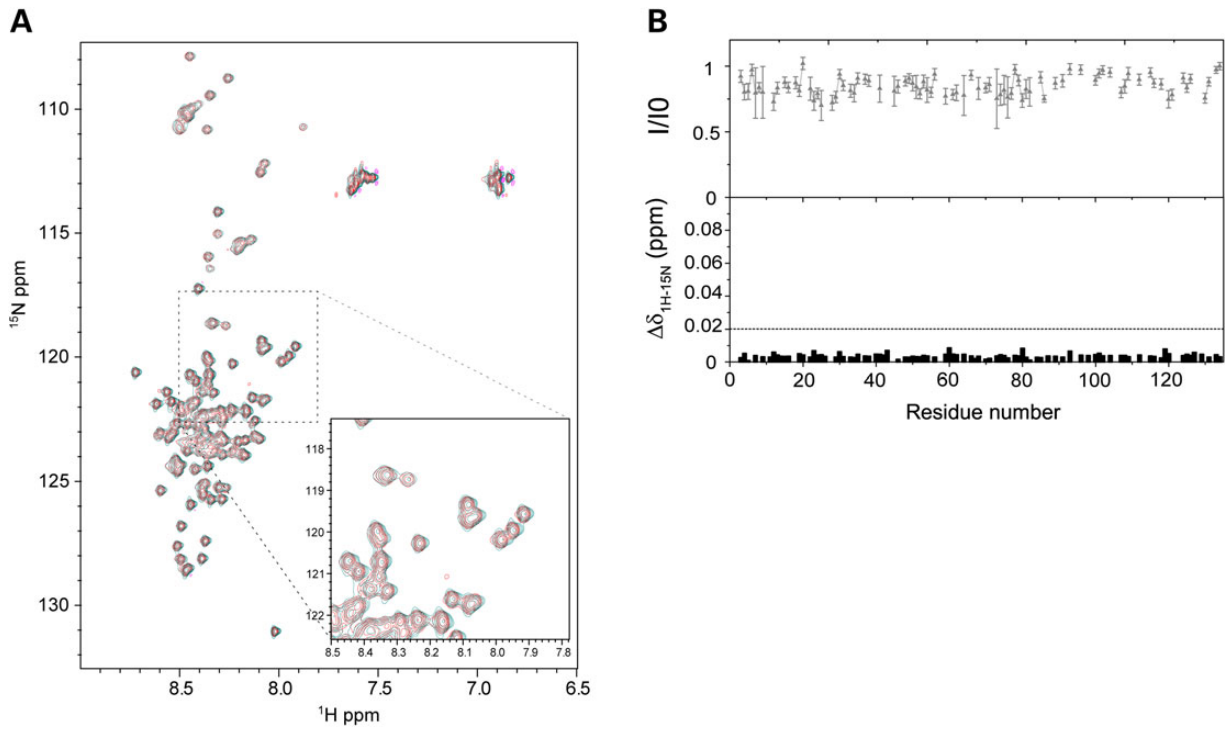

Figure 8. NMR characterization of the interaction between disordered aSyn and bSyn in solution. (**A**) 2D {^{1}H–^{15}N}-HSQC spectrum of {^{15}N}-labeled bSyn in the absence (green) and presence of a 2-fold excess of aSyn tagged with MTSL at position 90 (red). (**B**) (Top) The ratio of residue-specific NMR signal intensities observed in {^{1}H–^{15}N}-HSQC experiments of bSyn in the absence (I_0) and presence (I) of MTSL-tagged aSyn. Error bars were calculated on the basis of the signal-to-noise ratio in the spectra. (Bottom) {^{1}H–^{15}N} chemical shift perturbation in {^{15}N}-labeled bSyn after addition of 2 equivalents of aSyn. Chemical shift perturbations are below the estimated uncertainty (dashed line) in NMR signal positions. Together with the observation that I_0/I ratios are changed by <0.25 (top panel) upon addition of paramagnetic aSyn shows that monomeric aSyn and monomeric bSyn do not bind strongly to each other in solution.

would have to originate from an interaction of aSyn with bSyn. Using a similar approach, transient interactions between two aSyn molecules were previously reported (43). In the current study, we added a 2-fold excess of MTSL-tagged aSyn to the sample with ^{15}N-labeled bSyn and recorded a {^{1}H–^{15}N}-HSQC experiment. Superposition of the {^{1}H–^{15}N}-HSQC experiments of bSyn in the absence and presence of aSyn suggested that both the position and intensity of the NMR signals of bSyn was unchanged (Fig. 8A). This was further confirmed by the quantitative analysis of peak intensities and positions (Fig. 8B): no changes in peak position were detected. In addition, signal intensities in bSyn, which were corrected for dilution, were similar in the absence and presence of aSyn. The small deviations of <0.25 of the I/I_0 ratios from unity is most likely due to small changes in sample conditions during the titration. In particular, for a specific interaction between bSyn and aSyn a pronounced (I/I_0 ratio < 0.7) broadening of a distinct region of the bSyn sequence is expected. Taken together, this analysis shows that monomeric, disordered aSyn and bSyn have a low propensity to interact in solution, indicating that additional cofactors are required to trigger their interaction and aggregation in cells.

Discussion

The heterologous expression of human aSyn in yeast has been extensively used to obtain important insight into the molecular basis of PD and other synucleinopathies (35,36,38,44–47).

Despite the obvious similarity among the various members of the synuclein family, the biological effects of bSyn and gSyn were only recently assessed in greater detail (8,48). Here, we aimed to investigate the behavior of human bSyn and gSyn in yeast cells, upon heterologous expression. We observed that bSyn expression is also toxic in yeast, similarly to what is observed for aSyn (33,35). In contrast, expression human gSyn is not toxic, and no inclusions were formed at the levels of expression used in our study.

In yeast, expression of aSyn induces the accumulation of vesicles (45,46,49), raising the question of whether the fluorescent foci observed using microscopy are true aggregated forms of aSyn. However, we recently performed detailed biochemical characterization of the aSyn species formed in yeast cells and observed that, indeed, they correspond to the formation of high molecular weight species (36). Moreover, other studies showed that some of the inclusions formed by aSyn in yeast are thioflavin S or thioflavin T positive, indicating they have amyloid-like properties (50,51). Here, we took advantage of FRAP analysis and observed that inclusions formed by bSyn-GFP and aSyn-GFP have exactly the same dynamics indicating that they share the same biochemical nature.

We then investigated the mechanisms of toxicity associated with bSyn expression, asking whether these are similar to those associated with aSyn expression. Several studies in yeast revealed that aSyn impairs vesicular trafficking, and that this is a major component for aSyn-dependent toxicity (40,45,47). We found that, like aSyn, bSyn toxicity is also associated with ER-to-Golgi trafficking defects, as the bSyn toxicity could be rescued by overproduction of genes that increase forward transport between ER and Golgi (*YPT1*, *YKT6* and *UBP3*), while the overproduction of genes that negatively regulate ER-Golgi trafficking (*GYP8* and *PMR1*), exacerbate bSyn toxicity.

The expression of aSyn in yeast cells induces oxidative stress, which in turn contributes to cell death (37). How aSyn triggers ROS accumulation is not completely understood, but it has been proposed that it could be partially an indirect effect, as a consequence of mitochondrial dysfunction induced by aSyn (38). Interestingly, we observed that bSyn also increases the levels of superoxide radical in yeast cells.

The bSyn mutations V70M and P123H have been associated with rare sporadic and familial cases of DLBs, respectively (14). Here, we showed that the V70M and P123H mutations increase bSyn inclusion formation in yeast, in line with the observation that these mutations induce lysosomal inclusion formation in a neuroblastoma cell line (15). However, these mutations did not increase bSyn toxicity. Strikingly, in a transgenic mouse model expressing P123H bSyn, co-expression of aSyn was found to greatly enhance neurodegeneration (16). In our yeast model, co-expression of WT forms of aSyn and bSyn resulted in a severe growth phenotype, rendering impossible the evaluation of the effect of the co-expression of the bSyn mutants with aSyn. Nevertheless, our findings are of great significance as the occurrence of bSyn mutations is rather rare. In addition, our findings suggest that, increased levels of bSyn may aggravate aSyn-associated cytotoxicity and neurodegeneration, calling for in depth studies in synucleinopathy patients, and suggesting gene dosage alterations, due to multiplications or promoter polymorphisms in the bSyn gene, may play an important and previously unexplored role in these disorders.

PTMs constitute an essential level of regulation of protein folding, localization and function. Thus, many PTMs have been associated with numerous neurodegenerative disorders (29). In PD and other synucleinopathies, aSyn phosphorylation on S129 is the most studied modification (29). PLK2 and 3 are among the kinases known to phosphorylate aSyn S129 and were also found to phosphorylate bSyn on S118 (5). Although there is still no evidence exist that this modification might have a pathological role in humans, we found that the mutant of bSyn where phosphorylation is mimicked by the introduction of a negatively charged amino acid (S118D) is more toxic and forms a larger number of inclusions per cell, suggesting that this modification might be an important modulator of bSyn toxicity. Future *in vivo* studies in animal models will be essential to inform on the role of this PTM in bSyn in disease. The lack of a specific antibody that specifically recognizes this phosphorylation unable the evaluation of the phosphorylation status of bSyn in yeast cells. However, the results here obtained suggest that, in contrast to what we previously found for aSyn phosphorylation on S129 (36), S118 of bSyn is not significantly phosphorylated by yeast endogenous kinases, as the behavior of WT bSyn-GFP is more similar to that of the mutants where phosphorylation is blocked (S118A or S118G).

We observed that co-expression of aSyn and bSyn is toxic for yeast cells, and that this toxicity is similar to that observed when identical levels of aSyn or bSyn are expressed. Interestingly, we found that co-expression aSyn and bSyn results in an increase in the percentage of cells with inclusions when compared with that observed when aSyn or bSyn are expressed. In the conditions tested, based on the use of multicopy vectors, we consider that our observation is highly important, as it is well established that increased levels of aSyn, due to genetic or environmental factors, is a risk factor for PD. In particular, polymorphisms in the aSyn gene that result in higher levels of expression of the protein are risk factors for PD (52–54). Our results indicate that increased levels of bSyn may also play an additive effect on aSyn, similar to what is observed with increased levels of aSyn.

We also asked if aSyn and bSyn could co-aggregate in cells when both proteins are present. Indeed, we found that aSyn and bSyn form heterodimers both in yeast and human cells. To further evaluate if co-aggregation was due to a unique propensity of aSyn and bSyn to interact as monomeric proteins in solution, we performed NMR spectroscopy, because this technique is highly sensitive for even weak protein–protein interactions. While transient interchain interactions were previously observed between aSyn molecules (43), we did not observe a direct interaction between aSyn and bSyn, when the two proteins were in the monomeric, disordered state. The differences in interchain behavior might either be caused by differences in solution conditions or be a consequence of sequence differences between the two synucleins. Indeed, it is well known that a very high sequence similarity is required in order for two proteins to assemble together into amyloid fibrils. Taken together, our data suggest that cellular co-factors are required to promote co-aggregation of aSyn and bSyn in cells and thus contribute to synucleinopathies (48).

Previous findings indicated that bSyn could inhibit aSyn aggregation and play a neuroprotective role (11,12,55). However, more recent reports revealed that bSyn may not always be protective, in line with the results we now present. In particular, overexpression of human bSyn using adeno-associated viral vectors is neurotoxic, and results in the formation of proteinase K-resistant aggregates of bSyn in primary cultured neurons and in dopaminergic neurons in rat brain (8). Mutations in bSyn were linked to DLB and rendered the protein neurotoxic in transgenic mice (16). Also, fibrillation of bSyn is promoted by macromolecular crowding, metal ions and pesticides (13), all of which are thought to be associated with PD.

Thus, our findings suggest that, while bSyn might play a protective role in normal conditions, where it may interact with aSyn, it might also contribute to disease under pathological conditions that may involve increased levels or toxic environmental insults. Nevertheless, additional studies will be necessary to clarify the interplay between aSyn and bSyn in both physiological and pathological conditions.

Altogether, our study indicates that bSyn can exert cytotoxicity in a manner that is similar to that caused by aSyn. The novel yeast models developed herein can be further explored in powerful genetic screens to further dissect the origin of bSyn toxicity, providing additional insight into the molecular basis of synucleinopathies.

Materials and Methods

Yeast plasmids and strains

aSyn, bSyn gSyn sequences were cloned into the *SpeI-HindIII* sites of p426GPD, p423GAL or p426GAL yeast expression vectors (34), as described before (35) (Table 1). GFP fusions were constructed in the same vectors by inserting the GFP coding sequence as a *ClaI-XhoI* digested polymerase chain reaction (PCR) product in frame with aSyn, bSyn or gSyn (35) (Table 1). Positive constructs were verified by DNA sequencing. bSyn mutants V70M, P123H, S118D, S118A and S118G were generated by site directed mutagenesis of the corresponding plasmids.

Yeast plasmids expressing fusions of aSyn or bSyn to the N-terminal (VN) or C-terminal (VC) part of Venus (41) (VN-aSyn, VN-bSyn, aSyn-VC, bSyn-VC) were cloned into the *SmaI* site of p423GAL or p426GAL using GENEART Seamless cloning and assembly kit (Life technologies).

The genes encoding modifiers of aSyn toxicity *YPT1*, *YKT6*, *UBP3*, *GYP8* and *PMR1* were cloned as described before (36) in

Table 2. Strains used in this study

	Description	References
W303-1A	MATa; *can1-100*; *his3-11,15*; *leu2-3,112*; *trp1-1*; *ura3-1*; *ade2-1*	(57)
W303.1A Ypt1	W303.1A *pAG305GPD YPT1 LEU2+*	This study
W303.1A Ykt6	W303.1A *pAG305GPD YKT6 LEU2+*	This study
W303.1A Ubp3	W303.1A *pAG305GPD UBP3 LEU2+*	This study
W303.1A Gyp8	W303.1A *pAG305GPD GYP8 LEU2+*	This study
W303.1A Pmr1	W303.1A *pAG305GPD PMR1 LEU2+*	This study

pRS-based gateway vectors pAG305GAL (*YPT1*, *YKT6*, *UBP3*, *GYP8* and *PMR1*) (56) (Table 1). These plasmids were integrated in the W303.1A genome to generate new strains (Table 2).

Yeast transformations were carried out using a standard lithium acetate procedure and all the genome insertions were confirmed by two independent PCRs following standard procedures (58).

Yeast cultures

Yeast strains were grown in synthetic complete (SC) medium [6.7 g L^{-1} yeast nitrogen base (BD Biosciences), appropriate amino acid dropout mix (Sunrise Science Products) without the appropriate plasmid selection auxotrophy, uracil (URA) and leucine (LEU), and with 1% (w/v) raffinose or 1% galactose (w/v) as carbon source.

For aSyn, bSyn and gSyn expression induction experiments, yeast cells were pre-grown in SC-URA raffinose liquid media at 30°C, with orbital agitation for 24 h (doubling time: ~3 h). After 24 h, optical density (OD) at 600 nm (OD_{600nm}) was measured and yeast cells were diluted to a standardized $OD_{600nm} = 3 \times 10^{-3}$ (~2.5×10^5 cells/mL) in SC-URA raffinose liquid media (no repression of the galactose-inducible promoter) and grown at 30°C, with orbital agitation. After 24 h, OD_{600nm} was measured. The volume of yeast culture needed to inoculate a new culture with an initial standardized $OD_{600nm} = 0.4$ (~14×10^6 cells/mL) was centrifuged (1810 *g*, at 30°C for 4 min). Cells were then resuspended in SC-URA galactose liquid media and incubated at 30°C, with orbital agitation, for 6 h. Co-expression experiments were performed in the same way, using SC-URA-LEU liquid media with either raffinose or galactose as carbon source.

For growth assays on solid medium, cultures OD_{600nm} was normalized to 0.05 ± 0.005 and 1/3 serial dilutions from this first-cell suspension were prepared. Spots of 4 µl of each cell suspension were then spotted on plates containing SC-URA or SC-URA-LEU solid media with glucose (control) or galactose as carbon source and incubated at 30°C for 3 days.

Protein extraction and immunoblotting analysis

For total protein extraction, yeast cells were lysed in MURB buffer (50 mM sodium phosphate, 25 mM MES, pH 7.0, 1% sodium dodecyl sulphate (SDS), 3 M urea, 0.5% 2-mercaptoethanol, 1 mM sodium azide) supplemented with protease inhibitor cocktail, with glass beads (3 cycles of 30 s in the beadbeater and 5 min on ice). Cell debris was removed by centrifugation (10 000 g, 1 min, room temperature) after denaturation at 70°C and the supernatant was collected. Equal volumes of total protein, corresponding to the same number of cells (normalized based on OD_{600nm}) were loaded in the SDS–polyacrylamide gel electrophoresis (PAGE) for the detection of aSyn, bSyn or gSyn levels. Protein samples were heated for 10 min at 70°C and centrifuged at 10 000 *g* for 1 min before acrylamide gel loading.

After SDS–PAGE run, samples were transferred to a nitrocellulose membrane using a Trans-Blot Turbo transfer system (Bio-Rad), as specified by the manufacturer.

Immunoblotting was performed following standard procedures using the following antibodies: GFP (NeuroMab); aSyn (Santa Cruz), bSyn (Abcam) anti phosphoglycerate kinase [PGK (Life Technologies Corporation)] and GAPDH (Thermo scientific) was used as loading control.

The band intensity of the different immunoblots signals was estimated using the ImageJ software (NIH, Bethesda, MD, USA) and normalized against the corresponding PGK signal. In particular, aSyn-GFP, bSyn-GFP and gSyn-GFP levels were determined by calculating the ratio between GFP/PGK and normalized to the control (mean ± SD).

Fluorescence microscopy and FRAP experiments

The percentage of cells with aSyn-GFP, bSyn-GFP or gSyn-GFP inclusions were determined by fluorescence microscopy using a Zeiss Axiovert 200M (Carl Zeiss) widefield fluorescence microscope equipped with a cooled CCD camera (Roper Scientific Coolsnap HQ) to acquire images containing at least 400 cells per strain, which were then manually counted using ImageJ.

Yeast cells were grown as described above. After 6 h of expression induction in galactose medium cells were collected by centrifugation and resuspended in phosphate-buffered saline (PBS) and 0.5% low melting agarose on a microscope slide.

FRAP experiments were performed as described before (36), using a Zeiss LSM 710 inverted laser scanning confocal microscope equipped with a large incubator (Pecon, Erbach, Germany) maintained at 30°C. Images were acquired using a PlanApochromat 63×/1.4 objective. A series of 80 z-stacks consisting of 5 different focal planes spaced 0.7 µm apart (frame size 512 × 512, pixel width 91 nm and pixel time 4.44 µs) were acquired at intervals of 2 s with pinhole set to 1 Airy unit. In each FRAP experiment a single inclusion focused at the central focal plane of the z-stack was bleached using the 488 nm laser line at 100% laser transmission on a circular region of interest with a diameter of 8 pixels (0.35 µm radius) for 32 ms. For imaging, the transmission of the 488 nm laser was set to 0.3% of the bleach intensity.

Image processing and fluorescence intensity measurements were performed in ImageJ using an in-house developed macro as described before (36).

Flow-cytometry

Flow-cytometry was performed in a fluorescence-activated cell sorting BD LSRFortessa. Yeast cell membrane integrity was evaluated with PI staining. Yeast cells were incubated with PI 5 µg/mL for 15 min. As a positive control, cells boiled for 10 min were used (data not shown). Fluorescence intensity of aSyn-GFP or bSyn-GFP was measured in simultaneous using a 488 nm laser for excitation and a 502 LP mirror in conjunction with a 530/30 BP filter for detection (BD Biosciences, San Jose, CA, USA).

30 µM DHE (Molecular Probe, Life Technologies), for 15 min at 30°C, with agitation and protected from light (59). A minimum of 10 000 events were collected for each experiment. Data analysis was performed using the FlowJo software (Tree Star, Inc., Ashland, OR, USA). Results were expressed as MFI of a molecule.

Plasmids for mammalian cell culture

Plasmids encoding aSyn fusions with the N-terminal (VN) or C-terminal (VC) halves of Venus fluorescent protein were previously described (41,60). To generate the bSyn fusions (VN-bSyn and bSyn-VC), the aSyn plasmids were cut to remove the aSyn

cDNA, and the cDNA encoding for bSyn was cloned into the *Nhe*I and *Xho*I sites.

HEK293 cell culture and transfections

HEK293 cells were cultured at 37°C in DMEM medium supplemented with 5% FCS, and in a 5% CO_2 atmosphere. Cells were transfected in a 12-well plate, at 80% confluence, with Metafectene (Biontex, Germany) in a ratio of 2:1 with the different synuclein-constructs (Fig. 7A and B: VN-aSyn, aSyn-VC, VN-bSyn, b-Syn-VC; Fig. 7C: aSyn and bSyn-V5), according to the manufacturer's instructions.

Forty-eight hours after transfection, cells were harvested using radioimmunoprecipitation assay buffer containing 0.1% Triton X-100, 0.15 M NaCl, 50 mM Tris, pH 7.5, and a protease inhibitor cocktail tablet (1 tablet/50 ml) (Roche Diagnostics). Lysates were centrifuged at 18 400 *g* for 30 min at 4°C. Protein concentration was measured using the Bradford assay (Bio-Rad).

SDS–PAGE and western blotting

Forty micrograms of total protein were loaded onto 15% SDS gels and transferred to nitrocellulose membranes (Immobilon-FL-Membrane, Millipore, Billerica, MA, USA). Membranes were washed with Tris-based buffer (TBS), and blocked with 5% Skim milk in TBS-Tween for 1 h at room temperature. Membranes were then incubated overnight at 4°C with antibodies against synuclein (1:2000, Ab6176, pan-synuclein, Abcam, New England, USA) and with y-Tubulin (1:3000, Clone GTU-88, Sigma, USA). Following three washing steps with TBS-Tween, membranes were incubated with horseradish peroxidase-conjugated secondary antibodies (1:10 000, GE Healthcare) for 2 h at room temperature. The signal was then detected using Immobilon Western Chemiluminescent HRP Substrate (Millipore Corporation).

Immunocytochemistry and microscopy

Forty-eight hours after transfection, cells were washed with PBS and fixed with 4% paraformaldehyde. Cells were permeabilized with PBS/0.1% Triton X-100, blocked for 1 h with 1.5% bovine serum albumin and incubated overnight with the primary antibody for aSyn (1:1000, mouse ab610787, BD Transduction Laboratories, USA) and for V5 tag (1:1000, rabbit ab9116, Abcam, New England, USA). After three washes with PBS, the secondary antibodies anti-mouse IgG conjugated to Alexa Fluor 555 (A31570) and anti-rabbit IgG conjugated to Alexa Fluor 488 (A21206) (Molecular Probes, OR, USA) 1:1000 was added for 1 h at room temperature. Cell nuclei were stained with Hoechst dye (Hoechst 33258, Molecular Probes). Fluorescent images were captured using a Leica Microsystems microscope (Leica DMI 6000B, Wetzlar, Germany).

Recombinant protein expression and purification

Plasmids encoding aSyn and bSyn were expressed in *Escherichia coli* BL21 (DE3) cells. Protein expression and purification was performed as previously described (61). aSyn was conjugated at position 90 to the nitroxide tag MTSL following established protocols (62). The two proteins were then dialyzed against the same NMR buffer of 50 mM 4-(2-hydroxyethyl)-1-piperazineethanesulfonic acid, 0.02% NaN_3, pH 7.4. Experiments were performed on 700 NMR spectrometers (Bruker), equipped with cryogenic probes, at 288 K. NMR experiments were carried out by addition of a 2-fold excess of unlabeled, MTSL-tagged aSyn to {^{15}N}-labeled bSyn (100 μM). Before and after addition of aSyn, the pH of the sample was checked to exclude effects due to pH variation. Heteronuclear {^{1}H–^{15}N}-HSQC experiments were acquired with 2048(H)*256(N) complex points (63). Spectra were processed using Topspin (Bruker) and NMRPipe (64) and analyzed with ccpnmr Analysis 2.2.1 (65). For spectral analysis, the backbone assignment of bSyn as deposited in the Biological Magnetic Resonance Bank (66) was used. The combined {^{1}H–^{15}N} chemical shift perturbation according to:

$$\Delta\delta_{^{1}\mathrm{H}-^{15}\mathrm{N}} = \sqrt{\frac{(\Delta H)^2 + (\Delta N/5)^2}{2}}$$

Statistical analyses

Statistical analyses were performed using the SigmaStat 3.10 software. All data are reported as averages of three independent experiments ± standard deviation (SD). Differences between treatments were detected by one way analyses of variance (ANOVA) using Tukey honest significant difference multiple comparison test ($\alpha = 0.05$).

Supplementary Material

Supplementary Material is available at *HMG* online.

Acknowledgements

We thank António Temudo and Ana Margarida Nascimento for imaging support; Ana Vieira, Ana Sílvia Gonçalves and Zélia Silva for flow cytometry assistance.

Conflict of Interest statement. None declared.

Funding

This work was supported by Fundação para a Ciência e Tecnologia (grant PTDC/BIA-BCM/117975/2010, SFRH/BPD/101646/2014 to S.T. and IMM/BTI/91-2012 to R.R.R.). E.G., B.P., M.Z., G.H.B. and T.F. O. are supported by the DFG Center for Nanoscale Microscopy and Molecular Physiology of the Brain.

References

1. Lavedan, C. (1998) The synuclein family. *Genome Res.*, **8**, 871–880.
2. Greten-Harrison, B., Polydoro, M., Morimoto-Tomita, M., Diao, L., Williams, A.M., Nie, E.H., Makani, S., Tian, N., Castillo, P.E., Buchman, V.L. *et al.* (2010) alphabetagamma-Synuclein triple knockout mice reveal age-dependent neuronal dysfunction. *Proc. Natl. Acad. Sci. USA*, **107**, 19573–19578.
3. Vargas, K.J., Makani, S., Davis, T., Westphal, C.H., Castillo, P.E. and Chandra, S.S. (2014) Synucleins regulate the kinetics of synaptic vesicle endocytosis. *J. Neurosci.*, **34**, 9364–9376.
4. George, J.M. (2002) The synucleins. *Genome Biol.*, **3**, REVIEWS3002.
5. Mbefo, M.K., Paleologou, K.E., Boucharaba, A., Oueslati, A., Schell, H., Fournier, M., Olschewski, D., Yin, G., Zweckstetter, M., Masliah, E. *et al.* (2010) Phosphorylation of synucleins by members of the Polo-like kinase family. *J. Biol. Chem.*, **285**, 2807–2822.
6. Lashuel, H.A., Overk, C.R., Oueslati, A. and Masliah, E. (2013) The many faces of alpha-synuclein: from structure and toxicity to therapeutic target. *Nat. Rev. Neurosci.*, **14**, 38–48.
7. Spillantini, M.G., Crowther, R.A., Jakes, R., Hasegawa, M. and Goedert, M. (1998) alpha-Synuclein in filamentous inclusions

of Lewy bodies from Parkinson's disease and dementia with Lewy bodies. *Proc. Natl. Acad. Sci. USA*, **95**, 6469–6473.
8. Taschenberger, G., Toloe, J., Tereshchenko, J., Akerboom, J., Wales, P., Benz, R., Becker, S., Outeiro, T.F., Looger, L.L., Bahr, M. *et al.* (2013) beta-synuclein aggregates and induces neurodegeneration in dopaminergic neurons. *Ann. Neurol.*, **74**, 109–118.
9. Uversky, V.N., Li, J., Souillac, P., Millett, I.S., Doniach, S., Jakes, R., Goedert, M. and Fink, A.L. (2002) Biophysical properties of the synucleins and their propensities to fibrillate: inhibition of alpha-synuclein assembly by beta- and gamma-synucleins. *J. Biol. Chem.*, **277**, 11970–11978.
10. Fan, Y., Limprasert, P., Murray, I.V., Smith, A.C., Lee, V.M., Trojanowski, J.Q., Sopher, B.L. and La Spada, A.R. (2006) Beta-synuclein modulates alpha-synuclein neurotoxicity by reducing alpha-synuclein protein expression. *Hum. Mol. Genet.*, **15**, 3002–3011.
11. Hashimoto, M., Rockenstein, E., Mante, M., Mallory, M. and Masliah, E. (2001) beta-Synuclein inhibits alpha-synuclein aggregation: a possible role as an anti-parkinsonian factor. *Neuron*, **32**, 213–223.
12. Hashimoto, M., Rockenstein, E., Mante, M., Crews, L., Bar-On, P., Gage, F.H., Marr, R. and Masliah, E. (2004) An antiaggregation gene therapy strategy for Lewy body disease utilizing beta-synuclein lentivirus in a transgenic model. *Gene Ther.*, **11**, 1713–1723.
13. Yamin, G., Munishkina, L.A., Karymov, M.A., Lyubchenko, Y. L., Uversky, V.N. and Fink, A.L. (2005) Forcing nonamyloidogenic beta-synuclein to fibrillate. *Biochemistry*, **44**, 9096–9107.
14. Ohtake, H., Limprasert, P., Fan, Y., Onodera, O., Kakita, A., Takahashi, H., Bonner, L.T., Tsuang, D.W., Murray, I.V., Lee, V.M. *et al.* (2004) Beta-synuclein gene alterations in dementia with Lewy bodies. *Neurology*, **63**, 805–811.
15. Wei, J., Fujita, M., Nakai, M., Waragai, M., Watabe, K., Akatsu, H., Rockenstein, E., Masliah, E. and Hashimoto, M. (2007) Enhanced lysosomal pathology caused by beta-synuclein mutants linked to dementia with Lewy bodies. *J. Biol. Chem.*, **282**, 28904–28914.
16. Fujita, M., Sugama, S., Sekiyama, K., Sekigawa, A., Tsukui, T., Nakai, M., Waragai, M., Takenouchi, T., Takamatsu, Y., Wei, J. *et al.* (2010) A beta-synuclein mutation linked to dementia produces neurodegeneration when expressed in mouse brain. *Nat. Commun.*, **1**, 110.
17. Fujita, M., Sekigawa, A., Sekiyama, K., Takamatsu, Y. and Hashimoto, M. (2012) Possible alterations in beta-synuclein, the non-amyloidogenic homologue of alpha-synuclein, during progression of sporadic alpha-synucleinopathies. *Int. J. Mol. Sci.*, **13**, 11584–11592.
18. Clayton, D.F. and George, J.M. (1998) The synucleins: a family of proteins involved in synaptic function, plasticity, neurodegeneration and disease. *Trends Neurosci.*, **21**, 249–254.
19. Surgucheva, I., McMahan, B., Ahmed, F., Tomarev, S., Wax, M. B. and Surguchov, A. (2002) Synucleins in glaucoma: implication of gamma-synuclein in glaucomatous alterations in the optic nerve. *J. Neurosci. Res.*, **68**, 97–106.
20. Galvin, J.E., Giasson, B., Hurtig, H.I., Lee, V.M. and Trojanowski, J.Q. (2000) Neurodegeneration with brain iron accumulation, type 1 is characterized by alpha-, beta-, and gamma-synuclein neuropathology. *Am. J. Pathol.*, **157**, 361–368.
21. Galvin, J.E., Uryu, K., Lee, V.M. and Trojanowski, J.Q. (1999) Axon pathology in Parkinson's disease and Lewy body dementia hippocampus contains alpha-, beta-, and gamma-synuclein. *Proc. Natl. Acad. Sci. USA*, **96**, 13450–13455.
22. Peters, O.M., Shelkovnikova, T., Highley, J.R., Cooper-Knock, J., Hortobagyi, T., Troakes, C., Ninkina, N. and Buchman, V.L. (2015) Gamma-synuclein pathology in amyotrophic lateral sclerosis. *Ann. Clin. Transl. Neurol.*, **2**, 29–37.
23. Chen, L. and Feany, M.B. (2005) Alpha-synuclein phosphorylation controls neurotoxicity and inclusion formation in a Drosophila model of Parkinson disease. *Nat Neurosci.*, **8**, 657–663.
24. Smith, W.W., Margolis, R.L., Li, X., Troncoso, J.C., Lee, M.K., Dawson, V.L., Dawson, T.M., Iwatsubo, T. and Ross, C.A. (2005) Alpha-synuclein phosphorylation enhances eosinophilic cytoplasmic inclusion formation in SH-SY5Y cells. *J. Neurosci.*, **25**, 5544–5552.
25. Gao, H.M., Kotzbauer, P.T., Uryu, K., Leight, S., Trojanowski, J. Q. and Lee, V.M. (2008) Neuroinflammation and oxidation/nitration of alpha-synuclein linked to dopaminergic neurodegeneration. *J. Neurosci.*, **28**, 7687–7698.
26. Koob, A.O., Ubhi, K., Paulsson, J.F., Kelly, J., Rockenstein, E., Mante, M., Adame, A. and Masliah, E. (2010) Lovastatin ameliorates alpha-synuclein accumulation and oxidation in transgenic mouse models of alpha-synucleinopathies. *Exp. Neurol.*, **221**, 267–274.
27. Anderson, J.P., Walker, D.E., Goldstein, J.M., de Laat, R., Banducci, K., Caccavello, R.J., Barbour, R., Huang, J., Kling, K., Lee, M. *et al.* (2006) Phosphorylation of Ser-129 is the dominant pathological modification of alpha-synuclein in familial and sporadic Lewy body disease. *J. Biol. Chem.*, **281**, 29739–29752.
28. Fujiwara, H., Hasegawa, M., Dohmae, N., Kawashima, A., Masliah, E., Goldberg, M.S., Shen, J., Takio, K. and Iwatsubo, T. (2002) alpha-Synuclein is phosphorylated in synucleinopathy lesions. *Nat. Cell Biol.*, **4**, 160–164.
29. Tenreiro, S., Eckermann, K. and Outeiro, T.F. (2014) Protein phosphorylation in neurodegeneration: friend or foe? *Front. Mol. Neurosci.*, **7**, 42.
30. Mahul-Mellier, A.L., Fauvet, B., Gysbers, A., Dikiy, I., Oueslati, A., Georgeon, S., Lamontanara, A.J., Bisquertt, A., Eliezer, D., Masliah, E. *et al.* (2014) c-Abl phosphorylates alpha-synuclein and regulates its degradation: implication for alpha-synuclein clearance and contribution to the pathogenesis of Parkinson's disease. *Hum. Mol. Genet.*, **23**, 2858–2879.
31. Paleologou, K.E., Oueslati, A., Shakked, G., Rospigliosi, C.C., Kim, H.Y., Lamberto, G.R., Fernandez, C.O., Schmid, A., Chegini, F., Gai, W.P. *et al.* (2010) Phosphorylation at S87 is enhanced in synucleinopathies, inhibits alpha-synuclein oligomerization, and influences synuclein-membrane interactions. *J. Neurosci.*, **30**, 3184–3198.
32. Nakajo, S., Tsukada, K., Omata, K., Nakamura, Y. and Nakaya, K. (1993) A new brain-specific 14-kDa protein is a phosphoprotein. Its complete amino acid sequence and evidence for phosphorylation. *Eur. J. Biochem.*, **217**, 1057–1063.
33. Tenreiro, S., Munder, M.C., Alberti, S. and Outeiro, T.F. (2013) Harnessing the power of yeast to unravel the molecular basis of neurodegeneration. *J. Neurochem.*, **127**, 438–452.
34. Mumberg, D., Muller, R. and Funk, M. (1995) Yeast vectors for the controlled expression of heterologous proteins in different genetic backgrounds. *Gene*, **156**, 119–122.
35. Outeiro, T.F. and Lindquist, S. (2003) Yeast cells provide insight into alpha-synuclein biology and pathobiology. *Science*, **302**, 1772–1775.
36. Tenreiro, S., Reimao-Pinto, M.M., Antas, P., Rino, J., Wawrzycka, D., Macedo, D., Rosado-Ramos, R., Amen, T., Waiss, M., Magalhaes, F. *et al.* (2014) Phosphorylation modulates clearance of alpha-synuclein inclusions in a yeast model of Parkinson's disease. *PLoS Genet.*, **10**, e1004302.
37. Flower, T.R., Chesnokova, L.S., Froelich, C.A., Dixon, C. and Witt, S.N. (2005) Heat shock prevents alpha-synuclein-

induced apoptosis in a yeast model of Parkinson's disease. *J. Mol. Biol.*, **351**, 1081–1100.
38. Su, L.H.J., Auluck, P.K., Outeiro, T.F., Yeger-Lotem, E., Kritzer, J. A., Tardiff, D.F., Strathearn, K.E., Liu, F., Cao, S.S., Hamamichi, S. *et al.* (2010) Compounds from an unbiased chemical screen reverse both ER-to-Golgi trafficking defects and mitochondrial dysfunction in Parkinson's disease models. *Dis. Model Mech.*, **3**, 194–208.
39. Macedo, D., Tavares, L., McDougall, G.J., Vicente Miranda, H., Stewart, D., Ferreira, R.B., Tenreiro, S., Outeiro, T.F. and Santos, C.N. (2015) (Poly)phenols protect from alpha-synuclein toxicity by reducing oxidative stress and promoting autophagy. *Hum. Mol. Genet.*, **24**, 1717–1732.
40. Cooper, A.A., Gitler, A.D., Cashikar, A., Haynes, C.M., Hill, K.J., Bhullar, B., Liu, K., Xu, K., Strathearn, K.E., Liu, F. *et al.* (2006) Alpha-synuclein blocks ER-Golgi traffic and Rab1 rescues neuron loss in Parkinson's models. *Science*, **313**, 324–328.
41. Outeiro, T.F., Putcha, P., Tetzlaff, J.E., Spoelgen, R., Koker, M., Carvalho, F., Hyman, B.T. and McLean, P.J. (2008) Formation of toxic oligomeric alpha-synuclein species in living cells. *PLoS One*, **3**, e1867.
42. Bertoncini, C.W., Jung, Y.S., Fernandez, C.O., Hoyer, W., Griesinger, C., Jovin, T.M. and Zweckstetter, M. (2005) Release of long-range tertiary interactions potentiates aggregation of natively unstructured alpha-synuclein. *Proc. Natl. Acad. Sci. USA*, **102**, 1430–1435.
43. Wu, K.P. and Baum, J. (2010) Detection of transient interchain interactions in the intrinsically disordered protein alpha-synuclein by NMR paramagnetic relaxation enhancement. *J. Am. Chem. Soc.*, **132**, 5546–5547.
44. Gitler, A.D., Chesi, A., Geddie, M.L., Strathearn, K.E., Hamamichi, S., Hill, K.J., Caldwell, K.A., Caldwell, G.A., Cooper, A.A., Rochet, J.C. *et al.* (2009) alpha-Synuclein is part of a diverse and highly conserved interaction network that includes PARK9 and manganese toxicity. *Nat. Genet.*, **41**, 308–315.
45. Sancenon, V., Lee, S.A., Patrick, C., Griffith, J., Paulino, A., Outeiro, T.F., Reggiori, F., Masliah, E. and Muchowski, P.J. (2012) Suppression of -synuclein toxicity and vesicle trafficking defects by phosphorylation at S129 in yeast depends on genetic context. *Hum. Mol. Genet.*, **21**, 2432–2449.
46. Soper, J.H., Roy, S., Stieber, A., Lee, E., Wilson, R.B., Trojanowski, J.Q., Burd, C.G. and Lee, V.M.Y. (2008) alpha-synuclein-induced aggregation of cytoplasmic vesicles in *Saccharomyces cerevisiae*. *Mol. Biol. Cell*, **19**, 1093–1103.
47. Willingham, S., Outeiro, T.F., DeVit, M.J., Lindquist, S.L. and Muchowski, P.J. (2003) Yeast genes that enhance the toxicity of a mutant huntingtin fragment or alpha-synuclein. *Science*, **302**, 1769–1772.
48. Sekigawa, A., Takamatsu, Y., Sekiyama, K. and Hashimoto, M. (2015) Role of alpha- and beta-synucleins in the axonal pathology of Parkinson's disease and related synucleinopathies. *Biomolecules*, **5**, 1000–1011.
49. Gitler, A.D., Bevis, B.J., Shorter, J., Strathearn, K.E., Hamamichi, S., Su, L.J., Caldwell, K.A., Caldwell, G.A., Rochet, J.C., McCaffery, J.M. *et al.* (2008) The Parkinson's disease protein alpha-synuclein disrupts cellular Rab homeostasis. *Proc. Natl. Acad. Sci. USA*, **105**, 145–150.
50. Zabrocki, P., Pellens, K., Vanhelmont, T., Vandebroek, T., Griffioen, G., Wera, S., Van Leuven, F. and Winderickx, J. (2005) Characterization of alpha-synuclein aggregation and synergistic toxicity with protein tau in yeast. *FEBS J.*, **272**, 1386–1400.
51. Oien, D.B., Shinogle, H.E., Moore, D.S. and Moskovitz, J. (2009) Clearance and phosphorylation of alpha-synuclein are inhibited in methionine sulfoxide reductase a null yeast cells. *J. Mol. Neurosci.*, **39**, 323–332.
52. Pals, P., Lincoln, S., Manning, J., Heckman, M., Skipper, L., Hulihan, M., Van den Broeck, M., De Pooter, T., Cras, P., Crook, J. *et al.* (2004) Alpha-synuclein promoter confers susceptibility to Parkinson's disease. *Ann. Neurol.*, **56**, 591–595.
53. Tan, E.K., Chai, A., Teo, Y.Y., Zhao, Y., Tan, C., Shen, H., Chandran, V.R., Teoh, M.L., Yih, Y., Pavanni, R. *et al.* (2004) Alpha-synuclein haplotypes implicated in risk of Parkinson's disease. *Neurology*, **62**, 128–131.
54. Chiba-Falek, O., Kowalak, J.A., Smulson, M.E. and Nussbaum, R.L. (2005) Regulation of alpha-synuclein expression by poly (ADP ribose) polymerase-1 (PARP-1) binding to the NACP-Rep1 polymorphic site upstream of the SNCA gene. *Am. J. Hum. Genet.*, **76**, 478–492.
55. Park, J.Y. and Lansbury, P.T. Jr. (2003) Beta-synuclein inhibits formation of alpha-synuclein protofibrils: a possible therapeutic strategy against Parkinson's disease. *Biochemistry*, **42**, 3696–3700.
56. Alberti, S., Gitler, A.D. and Lindquist, S. (2007) A suite of Gateway cloning vectors for high-throughput genetic analysis in *Saccharomyces cerevisiae*. *Yeast*, **24**, 913–919.
57. Thomas, B.J. and Rothstein, R. (1989) Elevated recombination rates in transcriptionally active DNA. *Cell*, **56**, 619–630.
58. Wendland, J. (2003) PCR-based methods facilitate targeted gene manipulations and cloning procedures. *Curr. Genet.*, **44**, 115–123.
59. Owusu-Ansah, E., Yavari, A. and Banerjee, U. (2008) A protocol for *in vivo* detection of reactive oxygen species. *Protoc. Exchange*, doi: 10.1038/nprot.2008.1023.
60. Tetzlaff, J.E., Putcha, P., Outeiro, T.F., Ivanov, A., Berezovska, O., Hyman, B.T. and McLean, P.J. (2008) CHIP targets toxic alpha-Synuclein oligomers for degradation. *J. Biol. Chem.*, **283**, 17962–17968.
61. Hoyer, W., Antony, T., Cherny, D., Heim, G., Jovin, T.M. and Subramaniam, V. (2002) Dependence of alpha-synuclein aggregate morphology on solution conditions. *J. Mol. Biol.*, **322**, 383–393.
62. Fawzi, N.L., Fleissner, M.R., Anthis, N.J., Kalai, T., Hideg, K., Hubbell, W.L. and Clore, G.M. (2011) A rigid disulfide-linked nitroxide side chain simplifies the quantitative analysis of PRE data. *J. Biomol. NMR*, **51**, 105–114.
63. Mori, S., Abeygunawardana, C., Johnson, M.O. and van Zijl, P. C. (1995) Improved sensitivity of HSQC spectra of exchanging protons at short interscan delays using a new fast HSQC (FHSQC) detection scheme that avoids water saturation. *J. Magn. Reson. B*, **108**, 94–98.
64. Delaglio, F., Grzesiek, S., Vuister, G.W., Zhu, G., Pfeifer, J. and Bax, A. (1995) NMRPipe: a multidimensional spectral processing system based on UNIX pipes. *J. Biomol. NMR*, **6**, 277–293.
65. Vranken, W.F., Boucher, W., Stevens, T.J., Fogh, R.H., Pajon, A., Llinas, M., Ulrich, E.L., Markley, J.L., Ionides, J. and Laue, E.D. (2005) The CCPN data model for NMR spectroscopy: development of a software pipeline. *Proteins*, **59**, 687–696.
66. Bertoncini, C.W., Rasia, R.M., Lamberto, G.R., Binolfi, A., Zweckstetter, M., Griesinger, C. and Fernandez, C.O. (2007) Structural characterization of the intrinsically unfolded protein beta-synuclein, a natural negative regulator of alpha-synuclein aggregation. *J. Mol. Biol.*, **372**, 708–722.